Biogeosciences Discuss., https://doi.org/10.5194/bg-2018-503
Manuscript under review for journal Biogeosciences
Discussion started: 13 December 2018

Insights from year-long measurements of air-water CH_4 and CO_2 exchange in a coastal environment

Mingxi Yang*, Thomas G. Bell, Ian J. Brown, James R. Fishwick, Vassilis Kitidis, Philip D. Nightingale, Andrew P. Rees, Timothy J. Smyth

Plymouth Marine Laboratory, Prospect Place, Plymouth, UK PL1 3DH.
* Correspondence to M. Yang (miya@pml.ac.uk)

Abstract. Air-water CH_4 and CO_2 fluxes were directly measured using the eddy covariance technique at the Penlee Point Atmospheric Observatory on the southwest coast of the United Kingdom from September 2015 to August 2016. The high frequency, year-long measurements provide unprecedented detail into the variability of these Greenhouse Gas fluxes from seasonal to diurnal and to semi-diurnal timescales. Depending on the wind sector, fluxes measured at this site are indicative of air-water exchange in coastal seas as well as in an outer estuary. For the open water sector when winds were off the Atlantic Ocean, annual CH_4 emission averaged ~0.05 mmol m^{-2} d^{-1}. Open water CH_4 flux was near zero in December and January, probably due to reduced biological production of CH_4. At times of high rainfall and river flow rate, CH_4 emission from the estuarine-influenced Plymouth Sound sector was several times higher than emission from the open water sector. The implied CH_4 saturation, derived from the measured fluxes and a wind speed dependent gas transfer velocity parameterization, of over 1000% in the Plymouth Sound is within range of in situ dissolved CH_4 measurements near the mouth of the river Tamar. CO_2 flux from the open water sector was generally from sea-to-air in autumn and winter and from air-to-sea in late spring and summer, with an annual mean flux of near zero. CO_2 flux from the Plymouth Sound sector was more positive, consistent with a higher dissolved CO_2 concentration in the estuarine waters. A diurnal signal in CO_2 flux and implied dissolved pCO_2 are clearly observed for the Plymouth Sound sector and also evident for the open water sector during biologically productive periods. These observations suggest that coastal CO_2 efflux may be underestimated if the sampling strategy is limited to daytime only. Combining the fluxes with in situ dissolved pCO_2 measurements within the flux footprints allows us to estimate the CO_2 transfer velocity. The gas transfer velocity vs. wind speed relationship at this coastal location agrees reasonably well with previous open water parameterizations in the mean, but demonstrates considerable variability. We discuss the influences of biological productivity and bottom-driven turbulence on coastal air-water gas exchange.

1 Introduction

Biogeosciences Discuss., https://doi.org/10.5194/bg-2018-503
Manuscript under review for journal Biogeosciences
Discussion started: 13 December 2018

The tropospheric abundances of methane (CH_4) and carbon dioxide (CO_2), two of the most important Greenhouse Gases (GHGs), have been increasing over the last few hundred years primarily due to human activities (Hartmann et al. 2013). Highly dynamic estuarine and coastal regions can be important sources and sinks of these GHGs. Understanding the emissions and uptake of these gases by coastal waters and how they change is directly relevant to the fulfillment of the United Nations Framework Convention on Climate Change (UNFCCC) Paris 2016 agreement. We argue in this paper that eddy covariance (EC), with temporal resolution of tens of minutes to hours, is the best method for long-term monitoring of coastal air-sea CH_4 and CO_2 fluxes.

There has been much debate over the causes of the recent tropospheric CH_4 trend, from varying wetland (e.g. Pison et al. 2013; Schaefer et al. 2016; Nisbet et al. 2016) and fossil fuel (e.g. Helmig et al. 2016; Rice et al. 2016) emissions, to changes in the atmospheric oxidative capacity (e.g. Rigby et al. 2017). Terrestrial aquatic systems may be important sources of tropospheric CH_4 (e.g. Borges et al., 2015). Similarly, due to benthic methanogenesis, large surface CH_4 supersaturations of thousands of percent have been observed in estuaries (e.g. Upstill-Goddard et al., 2000; Middelburg et al., 2002). Consequently, estuaries and coastal seas tend to have much greater CH_4 emissions per unit area than the open ocean (Bange et al. 2006; Forster et al. 2009).

Due to both the 'solubility pump' and the 'biological pump', the surface ocean can be a net source or sink of CO_2, depending on location and time of the year (Khatiwala et al. 2013; Houghton 2003). Globally averaged, the open ocean is modelled to absorb about a quarter of the anthropogenic CO_2 emission (Le Quéré et al. 2015). Shelf seas, despite the relatively small area, support high primary productivity, cause a large drawdown of CO_2 in the mean (Frankignoulle and Borges, 2001; Chen et al. 2013), and might be responsible for as much as 10-40% of global oceanic carbon sequestration (Muller-Karger et al. 2005; Cai et al. 2006; Chen et al. 2009; Laruelle et al. 2010). Estuaries, on the other hand, are generally net sources of CO_2 for the atmosphere (e.g. Frankignoulle et al. 1998). The direction of net air-sea CO_2 flux is less certain in coastal areas that are influenced by riverine outflow and anthropogenic activities (Chen et al. 2013). Kitidis et al. (2012) showed a gradient of increasing air-to-sea CO_2 flux with distance offshore in the western English Channel. Modeling of the carbonate chemistry and hence CO_2 flux in the North Western European shelf is hindered partly because of the uncertain representation of riverine influence (Artioli et al. 2012). The shallow seas are predicted to become a greater net sink of CO_2 in the future due to rising atmospheric CO_2 and increasing inorganic nutrients (e.g. Andersson and Mackenzie, 2004).

To quantify the impacts of estuarine and coastal emissions on the atmospheric CH_4 and CO_2 burden, an indirect method requiring the inventories of air-sea concentration difference (ΔC) and the gas transfer velocity (K) is usually utilized: Flux = $K \bullet \Delta C$. Coastal areas tend to be highly dynamic, with typically greater spatial and temporal variability in physics and biology than the open ocean. This heterogeneity poses serious challenges to observational and modeling efforts aimed at constraining

coastal air-sea GHG fluxes. Dissolved gas concentrations may be affected by tides, currents, mixed layer processes, and benthic/pelagic interactions. The sheltered nature of the coastal seas, coupled with freshwater input, often result in stratification (e.g. Sims et al. 2017), where biological processes can more quickly modify the near-surface dissolved gas concentrations. Mixed layer dynamics can vary on a diurnal timescale, due for example to buoyancy forcing (e.g. Esters et al. 2018). The atmospheric concentrations of GHGs at coastal locations also vary as a function of wind direction, airmass history, and boundary layer processes (e.g. Yang et al. 2016a).

The transfer velocity (K) primarily depends on turbulence, and over the ocean is generally parameterized as a function of wind speed (e.g. Wanninkhof et al. 2009). Currents and resultant bottom-driven turbulence significantly affect gas exchange in shallow waters, resulting in K values that can be much higher than predicted based on wind speed alone (O'Connor and Dobbins, 1958; Borges et al. 2004; Ho et al. 2014). Variability in biogeochemistry could also affect K by changing the surface tension and modifying the turbulence at the air-sea interface. Pereira et al. (2016) observed a gradient of increased sea surface surfactant activity from the open sea towards the coast, which reduced the gas transfer velocity by approximately a factor of two in their laboratory tank simulations. Thus a wind speed-only dependent representation of K, incomplete for the open ocean (Wanninkhof et al. 2009), is possibly even less adequate for a coastal environment. Measuring the fluxes directly with the eddy covariance technique is an ideal way to study the many controlling factors of K in such dynamic and heterogeneous environments. It also allows us to test the appropriateness of the indirect GHG flux calculations. Furthermore, compared to shipboard EC observations, measuring fluxes from a stationary tower has the advantage of not requiring any motion correction on the winds (see Edson et al. 1998). This means that flux and K measurements at a coastal location are potentially more accurate, especially at high wind speeds when the motion correction for a moving platform would become large.

Only a few coastal stations exist worldwide that have reported air-sea CO_2 fluxes by EC on a long timescale, such as Östergarnsholm station in the Baltic Sea (Rutgersson et al. 2008); the Utö Atmospheric and Marine Research Station also in the Baltic Sea (Honkanen et al. 2018); and Punta Morro in Baja California, Mexico (Gutíerrez-Loza and Ocampo-Torres, 2016). In the case of the Östergarnsholm station, concurrent measurements of partial pressure of seawater CO_2 (pCO_2) from a nearby buoy allow for the determination of the CO_2 gas transfer velocity. Unfortunately the open-path sensors utilized at Östergarnsholm and Punta Morro (LI-7500, LI-COR Biosciences) could well be affected by a CO_2-H_2O spectral interference (Blomquist et al. 2014; Landwehr et al. 2014; Butterworth and Else, 2018), likely resulting in biased fluxes under conditions of significant latent heat flux. CH_4 sensors with sufficient measurement frequency and precision for the EC methods have only been developed in recent years (Yang et al. 2016b). We are not aware of any published long-term air-sea CH_4 fluxes by the EC method.

In this paper, we describe a year-long set of air-water CO_2 and CH_4 flux measurements by EC at the coastal Penlee Point Atmospheric Observatory. The high frequency fluxes allow us to characterize their variability across a range of time scales

(semi-diurnal to diurnal to seasonal). Combining these data with in situ observations of dissolved gas concentrations as well as supporting physical and biogeochemical measurements enables us to quantify the gas transfer velocity at this coastal location and examine its controls.

2 Experimental

The Penlee Point Atmospheric Observatory (PPAO, 50° 19.08' N, 4° 11.35' W; http://www.westernchannelobservatory.org.uk/penlee/) was established in May 2014 on the southwest coast of the United Kingdom. Understanding the controls of coastal air-sea exchange is one of the main scientific foci at this site. Yang et al (2016a, 2016b) demonstrated that the PPAO is a suitable location to measure air-sea exchange by the EC method.

2.1 Eddy covariance fluxes

Atmospheric CH_4 and CO_2 mixing ratios were measured at a frequency of 10 Hz using a Los Gatos Research (LGR) Fast Greenhouse Gas Analyzer (FGGA, enhanced performance model) between September 2015 and August 2016. As described in detail by Yang et al (2016a), two Gill sonic anemometers (Windmaster Pro and R3) are installed on a mast on the rooftop of PPAO (~18 m above mean sea level). For this paper, wind data from the Windmaster Pro sonic anemometer were used between September 2015 and March 2016. Since March 2016, wind data from the R3 sonic anemometer (not operational for the first 6 months of this annual study) were preferred because of its higher precision and better performance during heavy rain events.

The gas inlet tip, located ~30 cm below the Windmaster Pro sonic anemometer centre volume, is connected to the LGR via a ~18 m long PFA tubing (3/8'' outer diameter). First a scroll pump (BOC Edwards XDS-35i) until 16 October 2015 and then a rotary vane pump (Gast 1023) were used to pull sample air through the inlet tubing, an aerosol filter (2 µm pore size, Swagelok SS-6F-05), and the LGR. The aerosol filter became laden with sea salt over time and the filter elements were replaced approximately every ~2 months. As a result, the volumetric flow rate through the LGR varied between 23 and 78 LPM, which affected the lag time and the high frequency attenuation of the fluxes. The lag time was determined from a maximum lag correlation analysis between CO_2 and the instantaneous vertical wind velocity (w), varing from about 2.7 to 9.0 s. The strong atmosphere-biosphere flux of CO_2 when winds were from land aided our determination of this lag time. The high frequency flux attenuation was estimated from the instrument response time (see Yang et al. 2013, 2016a) and a wind speed dependent correction was applied to the flux data (representing ~15% gain in the mean).

Fluxes of CH_4 and CO_2 were initially computed in 10-minute intervals from the covariance of their lag-shifted dry mixing ratios and w. Wind velocities were streamline corrected using the standard double rotation method (Tanner and Thurtell, 1969) on a 10-minute basis. Evaluations of the EC momentum transfer against the expected rate (Figure S2 in Supplementary

materials), as well as stationarity in winds and gas mixing ratios, are used to quality control the 10-minute flux data. The filtered 10-minute fluxes are further averaged to hourly and also six-hourly intervals to reduce random noise. See Yang et al. (2016a, 2016b) for further details on data processing, quality control, and measurements of momentum and sensible heat fluxes. Horizontal wind speed measurements are corrected for flow distortion and adjusted to a neutral atmosphere at 10-m height (see Supplementary Materials).

2.2 Flux footprints

The theoretical flux footprint model of Kljun et al. (2004) predicts the upwind distance of maximum flux contribution (X_{max}) and the distance of 90% cumulative flux contribution (X_{90}). . The semi-diurnal tidal range at this location is large (up to 6 m during spring tide), effectively raising the EC measurement height above water at low tide and reducing it at high tide. We combine the measurement height above mean sea level (18 m) with tidal height variations and the Kljun et al (2004) model (run in a neutral atmosphere) to estimate X_{max} and X_{90} as approximately 0.4 and 1.1 km at the highest tide and 0.6 and 1.6 km at the lowest tide. Stable and unstable atmospheres are predicted to increase and decrease X_{max} as well as X_{90}, respectively.

In this paper we focus on air-water transfer over two different wind sectors. When winds are from the southwest (180-240°), the eddy covariance flux footprint is over open water with a depth of approximately 20 m at X_{max}. When winds are from the northeast (45-80°), the footprint is over the fetch-limited Plymouth Sound (upwind distance of 5-6 km), which is ~10 m deep and significantly influenced by the outflow of the Tamar estuary (Siddorn et al. 2003; Uncles et al. 2015). See Supplementary material Figure S1 for a map of the site and the approximate flux footprints.

2.3 Seawater measurements

We used the Plymouth Marine Laboratory's Research Vessels (RV) *Quest* and *Plymouth Explorer* to study the spatial heterogeneity in this coastal environment. Underway seawater measurements on the *Quest* from ~3 m depth include pCO_2 (Kitidis et al. 2012), salinity, temperature, chlorophyll, and dissolved oxygen. As a part of the Western Channel Observatory sampling program (http://www.westernchannelobservatory.org.uk), the *Quest* made approximately weekly trips to the L4 station (50° 15.0' N, 4° 13.0' W; ~6 km south of PPAO) and fortnightly trips to the E1 station (50° 02.6' N, 4° 22.5' W; ~20 km south of PPAO). These visits were always during the daytime. On the way back to Plymouth from L4 and E1, the *Quest* often idled at about 600 m to the south/southwest of PPAO for approximately 10 minutes, enabling the collection of underway measurements within the open water flux footprint of PPAO. The ship also passed through the Plymouth Sound flux footprint of PPAO en route back into port.

Seawater samples were taken at the L4 station from a CTD rosette. For CH_4 analysis discrete seawater samples were collected directly from Niskin bottles using clean Tygon tubing into 500ml borosilicate bottles. Sample bottles were overfilled by three times their volume to eliminate air bubbles, poisoned with 100µl of a saturated mercuric chloride solution and returned to the laboratory where they were transferred to a water bath at 25°C and temperature equilibrated for a minimum of one hour before analysis. Samples were analysed for CH_4 by single-phase equilibration gas chromatography using a flame ionisation detector similar to that described by Upstill-Goddard et al. (1996). Samples were typically analysed at PML within 2 weeks of collection and calibrated against three certified (±5%) reference standards (Air Products Ltd), which are traceable to NOAA WMO-N2O-X2006A.

The other PML vessel (a hard-bottomed RHIB, *Plymouth Explorer*) was used to occasionally sample the estuary Tamar from the upper freshwater section near Gunnislake to the lower saltwater section near the Plymouth Sound in 2017 and 2018. This is a part of the NERC-funded LOCATE (Land Ocean Carbon Transfer; http://www.locate.ac.uk) research programme. Discrete seawater samples were collected at stations from the near surface into 500ml borosilicate bottles with care taken to eliminate air bubbles. Analysis for dissolved CH_4 was performed as described above.

3 Results

Over the one year of measurements, variability in physical and biogeochemical parameters was large: wind speed at times exceeding 20 m s^{-1}, seawater temperature varying between about 7 and 18°C, and chlorophyll a concentration ranging between about 0.2 and 5 mg m^{-3}. Time series of ancillary data (meteorological parameters, Tamar river flow, and surface ocean physical and biogeochemical parameters) are shown in the Supplementary materials (Figures S3 to S6). This region can be roughly generalized by a windier, wetter autumn and winter, and a calmer, dryer spring and summer. Southwesterly winds off the Atlantic Ocean (annual mean wind speed of ~8 m s^{-1}) occurred more frequently in the winter months, resulting in higher precipitation rates and greater riverine discharge. During southwesterly conditions, the temperatures in the sea surface and air were similar throughout the entire year, resulting in fairly small air-sea temperature difference and modest sensible heat fluxes (monthly average of typically -20 to 20 W m^{-2}). As a result, the atmosphere was generally close to neutral stability (monthly mean Monin-Obukhov stability parameter z/L between -1.7 and 0.04).

3.1 CH_4 fluxes

Figure 1 shows the air-sea flux of CH_4 over the one-year measurement period. Flux data gaps are due to either wind direction outside of air-water sectors or instrumental failure. As shown by Yang et al. (2016b), under ideal conditions (moderate winds and steady atmospheric mixing ratio) the random noise in the LGR CH_4 flux is on the order of 0.02 and 0.01 mmol m^{-2} d^{-1}

for one-hour average and six-hour average, respectively. In comparison, the standard deviation (σ) in the six-hour averaged CH_4 flux for the open water sector is about 0.05 mmol m^{-2} d^{-1} (computed over the entire year). Thus much of the rapid temporal fluctuations in the measured CH_4 flux appear to be driven by natural variability (due to changes in watermass within the flux footprint, wind, etc.), rather than due to random measurement noise. The semi-diurnal variability in CH_4 flux as a result of the tide is discussed in Section 3.3.

To more clearly illustrate the seasonal variability, the means and 25/75 percentiles of the six-hour averaged CH_4 fluxes are computed in monthly intervals (Figure 2). CH_4 flux was consistently positive, indicating emission of CH_4 from these coastal waters. The only exception was during the months of December and January, when CH_4 flux was near zero. The annual mean CH_4 flux from the open water sector was 0.047 (standard error, or SE of 0.008) mmol m^{-2} d^{-1} when computed from monthly mean fluxes and 0.039 (SE of 0.003) mmol m^{-2} d^{-1} when directly computed from six-hour mean fluxes. The second approach has a temporal bias because the frequency of appropriate wind directions that enable air-sea flux measurements is not the same during the year. For example, southwest winds were less frequent in spring (30% of time in March-May 2016) than in winter (60% of time in January 2016). Thus the annual means computed directly from six-hour fluxes are skewed by periods of extended measurements (although the results of the two approaches are not significantly different, with $p>0.05$). The annual mean CH_4 flux here is consistent with previous coastal estimates (e.g. Upstill-Goddard et al. 2016) and roughly an order of magnitude greater than estimated for the open ocean (e.g. Forster et al. 2009).

CH_4 flux from the Plymouth Sound sector was noticeably higher than flux from the open water sector, with an annual mean of about 0.108 (SE of 0.026) mmol m^{-2} d^{-1}. This enhancement in the flux was particularly noticeable at times of high rainfall and river discharge rate, with fluxes over 0.2 mmol m^{-2} d^{-1} in February 2016. During the dry summer months of 2016 (May and June), CH_4 fluxes from the two wind sectors were comparable. Northerly winds occurred only 7.4% of the time overall during the one-year study period. Thus the seasonal variability in CH_4 emission from the Plymouth Sound is less well represented than emission from the open water sector.

We briefly compare our measured fluxes with existing estimates of riverine CH_4 emission. The 1-km^2 resolution UK National Atmospheric Emissions Inventory (NAEI, http://naei.defra.gov. uk) reports a natural CH_4 emission source of 0.17 mmol m^{-2} d^{-1} averaged over the area of the Plymouth Sound for year 2013. Our annual mean flux from the Plymouth Sound wind sector is about 64% of the NAEI estimate. Based on in situ measurements of dissolved CH_4 concentrations in six major UK estuaries, Upstill-Goddard et al. (2016) estimated CH_4 emissions of 4.3 Gg yr^{-1} for UK outer estuaries (using a total outer estuarine area of 1894 km^2). If we crudely assume that the Plymouth Sound is a representative outer UK estuary, scaling up our mean flux from this wind sector to the total outer estuarine area of 1894 km^2 yields an annual flux of 1.2 Gg yr^{-1}. This is a lower than the estimate from Upstill-Goddard et al. (2016), likely because according to their survey the CH_4 saturation from the Tamar

is fairly low compared to some of the other major UK estuaries. The UK has a 12429 km long coastline. If the PPAO open water footprint is representative of the nearest 1.4 km (i.e. X_{90} of our fluxes, see Section 2.2) of the UK coast, our measurements extrapolate to a total CH_4 flux of 4.8 Gg yr^{-1} in UK coastal seas. We are not able to use PPAO EC flux data to provide estimates for CH_4 emission from the inner estuary, where fluxes might be the highest per unit area (Upstill-Goddard et al. 2016).

3.2 CO_2 fluxes

Figure 3 shows the air-sea flux of CO_2 over the one-year measurement period. The random noise in the LGR CO_2 flux is on the order of 4 and 2 mmol m^{-2} d^{-1} for one-hour average and six-hour average, respectively (Yang et al. 2016b). The standard deviation in the six-hour averaged CO_2 flux for the open water sector is about 20 mmol m^{-2} d^{-1} (computed over the entire year), substantially greater than the instrumental noise. Ambient variability (in e.g. dissolved concentrations) largely drives the rapid temporal fluctuations in CO_2 flux, which is unlikely to be fully captured by weekly or monthly seawater sampling.

The means and 25/75 percentiles of the six-hour averaged CO_2 fluxes are computed in monthly intervals (Figure 4). CO_2 flux from the open water sector was generally from sea-to-air in autumn and winter (up to 37 mmol m^{-2} d^{-1}) and from air-to-sea in spring and early-summer (as much as -26 mmol m^{-2} d^{-1}). The seasonality in CO_2 flux here is consistent with seawater pCO_2 observations by Litt et al. (2010) and Kitidis et al. (2012) from the same region. CO_2 flux from the Plymouth Sound sector appeared to be more positive than from the open water sector in some months.

A three-day time series of CO_2 flux from July 2016 is shown in Figure 5A. Winds were consistently from the southwest during this period, varying from about 3 to 12 m s^{-1} (Figure 5C). CO_2 flux during this period was clearly different between day (mean of about -13 mmol m^{-2} d^{-1}) and night (mean of about +9 mmol m^{-2} d^{-1}). Daytime pCO_2 measurements on the *Quest* imply a ΔpCO_2 of about -40 µatm and a net flux into the water. The EC flux is consistent in sign with ΔpCO_2 during the day, but not at night. The computed transfer velocity of CO_2 ($K_{CO2,660}$, see Section 5) using the interpolated daytime pCO_2 measurements yielded positive values during the day (as expected), but negative values at night (which is not physically possible). The positive CO_2 flux at night is unlikely to be caused by a nocturnal flux footprint that overlaps with land because both sensible heat and CH_4 fluxes are consistent with air-sea exchange. The air temperature was about 1.2 °C warmer than the water temperature, implying a slightly stable atmosphere and a flux footprint that extends further upwind from the PPAO site than in a neutral atmosphere (Kljun et al. 2004). The measured sensible heat flux averaged -9 W m^{-2} and showed little diurnal variability, consistent with the air-sea temperature difference. Similarly, CH_4 flux was positive (sea-to-air) and did not vary with the time of day.

The most likely reason for the negative nighttime $K_{CO2,660}$ is that seawater pCO_2 varied diurnally, probably due to a combination of biological and dynamical processes. Wind speed was generally higher at night during these few days and the measured fluxes imply that ΔpCO_2 (see next sections on this calculation) changed from about -40 µatm during the day to about 15 µatm at night. Similar diurnal cycles (with slightly reduced magnitudes) have been observed in high frequency pCO_2 measurements in the western English Channel by Marrec et al. (2014) and Litt et al. (2010). We note that a daytime CTD cast on 12th July 2016 showed a mixed layer at the L4 station of only ~10 m depth. Entrainment of deeper water could contribute towards a higher surface pCO_2 at night. A diurnal cycle in CO_2 flux was not obvious during times of expected evasion (sea-to-air flux). These periods of positive CO_2 flux occurred in autumn and winter when biological productivity was low and the water column was mixed to the bottom.

The annual mean CO_2 flux was 3.9 (SE of 4.9) mmol m^{-2} d^{-1} when computed from monthly mean fluxes (Figure 4) and 1.3 (SE of 1.3) mmol m^{-2} d^{-1} when directly computed from six-hour mean fluxes. If we sub-sample our EC observations to the period of 10:00–16:00 UTC only, the annual mean CO_2 flux becomes 2.5 (SE of 4.9) mmol m^{-2} d^{-1} when computed from monthly mean fluxes and -1.0 (SE of 2.2) mmol m^{-2} d^{-1} when directly computed from six-hour mean fluxes. These results highlight the value of our continuous flux measurements and suggest that CO_2 flux estimates based only on daytime pCO_2 measurements may be biased towards greater seawater net uptake for coastal environments such as the western English Channel.

3.3 Implied seawater CH_4 concentrations and saturations from fluxes

We wish to disentangle the processes that control the gas transfer velocity (K) from the processes that control the air-water concentration difference (ΔC). We first compute the implied seawater CH_4 and CO_2 concentrations from the eddy covariance fluxes by assuming a parameterization of gas transfer velocity. Here the sea-minus-air concentration difference is computed by dividing the EC flux by the wind speed-dependent transfer velocity from Nightingale et al. (2000) (adjusted for ambient Schmidt number by the exponent of -0.5). Adding the atmospheric concentration to ΔC yields the implied seawater concentration. To avoid excessive noise from dividing by a small K, implied seawater concentrations at wind speeds lower than 5 m s^{-1} are discarded.

Implied seawater CH_4 concentration from the open water flux footprint ranges from about 3 to 26 nM on a monthly interval (mean of 14 nM; see Figure 6). It is often convenient to represent dissolved CH_4 as a saturation level relative to the atmosphere (saturation = CH_{4w} / (CH_{4a} •sol_{CH4}) •100, where CH_{4w} and CH_{4a} are waterside and airside concentrations; sol_{CH4} is solubility as a function of temperature and salinity from Wanninkhof 2014). The lowest implied CH_4 concentration occurred in winter and corresponded to a saturation level of close to 100%. The highest implied CH_4 concentration was from April to November, with an average saturation level of about 600%. The solubility of CH_4 varies by only ~14% from summer to winter

at this location. Thus the seasonal variability in CH_4 concentration and saturation seems more likely to be due to changing biological processes (methanogenesis and/or CH_4 oxidation) and hydrodynamics than to dissolution (i.e. seasonal temperature changes). For the Plymouth Sound flux footprint, the implied concentration ranges from 9 to 99 nM (mean of 37 nM, corresponding to about 1200% saturation), with the highest values in late winter and early spring. We compare these implied concentrations and saturations with nearby dissolved CH_4 measurements in Section 4.3.

Based on measurements from April to June 2015 at PPAO, Yang et al. (2016a) observed that CH_4 flux from the open water flux footprint varied with the timing of the tide, but not with the tide height. Specifically, CH_4 flux tended to be the highest during the first ~4 hours after low water. This was attributed to the outflow of a lower salinity surface layer from the Tamar river and estuary during rising tide around the Penlee headland. A subtle semi-diurnal variability in CH_4 flux can be seen in Figure 5B. The same pattern is apparent over an annual cycle in the implied saturation level of CH_4. On average, CH_4 saturation within the open water sector was about 40% higher during rising tide than during falling tide.

3.4 Implied seawater CO_2 concentrations and saturations from fluxes

Monthly averaged implied seawater CO_2 concentrations from the two flux footprints are shown in Figure 7. For the open water sector, the greatest supersaturation in CO_2 is observed in late autumn, with values exceeding 500 µatm. The greatest undersaturation in CO_2 is observed in late spring and early summer, coinciding with an increase in chlorophyll a concentration at the nearby L4 station (Figure S6). On average, implied pCO_2 within the Plymouth Sound is 32 µatm higher than pCO_2 within the open water flux footprint, as might be expected given previous observations of supersaturated pCO_2 in the river Tamar (Frankignoulle et al. 1998).

Averaged over the entire year, implied seawater CO_2 saturation for the open water sector was about 100% in the daytime and slightly higher at night (Figure 8). In contrast, a marked diurnal variability in CO_2 saturation was observed for the Plymouth Sound sector, with a higher saturation level at night than during the day. Compared to the open water sector, the Plymouth Sound is more sheltered and influenced by the Tamar outflow, thus subject to greater near surface stratification and possibly different biological processes. The diurnal variability we observed is important in the context of estuarine CO_2 (and carbonate system) observations that are predominantly carried out during daytime when sampling and navigation are easier. Our findings suggest that such observations may underestimate estuarine pCO_2 and by extension the efflux of CO_2 to the atmosphere.

Interestingly, a semi-diurnal variability as a result of tide is not obvious in the implied CO_2 saturation. This could be because the influence of Tamar estuary on the PPAO flux footprint is less in terms of pCO_2 (e.g. due to the already large burden of carbonate and bicarbonate in seawater), and more on physical and biogeochemical processes. The diurnal variability in pCO_2 might also be confounding any semi-diurnal tidal signal.

It is worth noting that our implied seawater GHG concentrations would be overestimated if the actual gas transfer velocity is higher than the wind speed dependent parameterization of Nightingale et al. (2000). For example, bottom-driven turbulence could enhance the gas transfer velocity (e.g. Borges et al. 2004; Ho et al. 2014). We discuss the effects of depth and current velocity on gas exchange in Section 5.4.

4 Spatial variability in seawater concentrations

The estimation of the gas transfer velocity *K* requires concurrent measurements of flux and seawater concentration within the flux footprint. Typically dissolved pCO_2 was measured once or twice a week, and only some of the measurements were made within the PPAO flux footprints. Measurements of dissolved CH_4 were even scarcer and unfortunately none of them were made within the flux footprints. Thus in order to relate the high frequency EC fluxes with the discrete in situ dissolved gas concentrations, we first evaluate the spatial homogeneity of our study region the shipboard seawater measurements.

4.1 Variability in salinity

Previous modeling studies (Siddorn et al. 2003; Uncles et al. 2015) show that freshwater discharge from the Tamar estuary mainly flows along the western edge of Plymouth Sound and bends around PPAO towards the southwest. In Figure 9, we compare underway salinity measured within the PPAO flux footprints (open water to the southwest as well as the Plymouth Sound to the northeast) with near-coincidental *Quest* observations at the L4 station (6 km south of PPAO). Compared to the L4 station, mean salinity was 1.2 % and 2.1% lower in the open water and Plymouth Sound footprints, respectively. Periods of the lowest salinity both within the footprints and at L4 coincided with the greatest outflow from the Tamar estuary. These observations indicate that the Tamar outflow influences this entire region, and unsurprisingly water is generally fresher within the Plymouth Sound than in the open water flux footprint. We next assess how much this riverine outflow affects the dissolved CO_2 and CH_4 concentrations within the flux footprints of PPAO and thus the measured fluxes.

4.2 Variability in dissolved pCO_2

The underway in situ pCO_2 measured within the PPAO flux footprints is compared with the near-coincidental observations from the *Quest* at the L4 station in Figure 10. The highest pCO_2 measured both within the footprints and at L4 were observed at times of large riverine discharge. This is seemingly consistent with a Tamar influence (e.g. Frankignoulle et al. 1998) but is primarily driven by the seasonality in pCO_2 (Kitidis et al. 2012). Unlike salinity, the limited pCO_2 measurements within both flux footprints were very similar to pCO_2 at the L4 station. As shown in Figures S7-S9 of the Supplementary materials, fast responding sea surface temperature and chlorophyll a were not noticeably different between the footprints and L4,

while dissolved oxygen was lower within the flux footprints than at L4. It could be that the large burden of carbonate and bicarbonate in seawater partially buffered the impact of the freshwater input on pCO_2 within the flux footprints. We also note that the pCO_2 measurement with a 'shower head' equilibrator has an integration time of 8 minutes (Kitidis et al., 2012). The *Quest* usually only idled for ~10 minutes within the open water flux footprint and did not idle within the Plymouth Sound footprint. Thus it is possible that spatial variability was under represented in some of the pCO_2 measurements due to the fairly slow response time of the equilibrator.

In situ pCO_2 measurements from the Plymouth Sound footprint and from the open water footprint (plus L4, since they are not distinguishable) are shown in Figure 7, along with the 100% saturation value with respect the atmosphere. Implied pCO_2 for the open water sector and the in situ pCO_2 within the open water footprint (plus L4) broadly agree. Limiting the implied pCO_2 to daytime only further improves the agreement with the in situ pCO_2 measurements, which were made only during the day (see Section 3.2). These observations suggest that the direct impact of the Tamar outflow on pCO_2 in the open water flux footprints at PPAO is fairly small relative to the air-sea concentration difference as well as other sources of variability.

4.3 Variability in dissolved CH_4

Dissolved CH_4 was not measured within either flux footprint of PPAO. Here we look at how our implied CH_4 concentration from the fluxes compare to measurements of dissolved CH_4 in the river Tamar and at L4. On four separate days in April 2017, July 2017, January 2018, and April 2018, the *Plymouth Explorer* was used to sample from the upper reaches of Tamar to the seaward end of the River Tamar during a falling tide for dissolved CH_4 concentration. As shown in Figure 11, CH_4 in the estuarine part of the Tamar in general correlated inversely with salinity. For example, in April 2017 the CH_4 concentration was 491 nM at a salinity of 4.7 (upper Tamar), 274 nM at a salinity of 29.3 (lower Tamar), 15 nM at a salinity of 34.2 (at the mouth of the Tamar in the Plymouth Sound), and 2.4 nM at a salinity of 35.2 (L4). These correspond to CH_4 saturation values of ~10000% at a salinity of 29.3 and ~600% at a salinity of about 34.2 during this transect. The highest measured CH_4 were in July 2017 following heavy rainfall, with saturation of 6040% in the lower Tamar. In contrast, relatively low CH_4 were observed in January and April 2018. The measurements from the river Tamar in 2001 by Upstill-Goddard et al. (2016) are within the range of these more recent transects. Long-term observations of surface dissolved CH_4 at L4 between October 2013 and July 2017 indicate a mean ($\pm\sigma$) saturation of 123 ± 60%.

The implied seawater CH_4 concentrations for the Plymouth Sound sector (Section 3.3) are within range of the in situ measurements in the lower Tamar and near the Plymouth Sound. In contrast, implied seawater CH_4 concentrations for the open water sector are on average about four higher than the in situ measurements at L4. Thus, while pCO_2 within the open water flux footprint of the PPAO agrees reasonably well with pCO_2 at L4, this is very likely not the case for CH_4. The differences in

salinity (Figure 9) and in dissolved oxygen (Figure S9) indicate that the water masses within the flux footprints and at L4 are not identical.

Two features of the CH_4 concentration vs. salinity relationship are particularly relevant for the interpretation of our CH_4 flux measurements. First, the variability in dissolved CH_4 concentration in the Tamar is very large. For example, CH_4 concentration at a salinity of about 30 varies by a factor of 40 during the six transects. Even for measurements in the same month (April 2001, 2017, 2018), the variation in CH_4 concentrations at this salinity is by a factor of 12. Secondly, the horizontal gradient in CH_4 concentration near the mouth of the Tamar estuary is very steep. Observations from April and July 2017 show a slope of about -20 to -50 nM per salinity unit. Between September 2015 and August 2016, salinity within the open water flux footprint varied between 32.2 and 35.2, while salinity within the Plymouth Sound flux footprint varied between 32.0 and 35.1. The large range in CH_4 concentration and the strong and variable CH_4 vs. salinity relationship make any salinity-based prediction of dissolved CH_4 concentration within the flux footprints highly uncertain. Thus we focus on estimating the transfer velocity of CO_2, but not CH_4 in the next section.

5 Estimation of the CO_2 gas transfer velocity

The implied pCO_2 from EC fluxes in monthly bins and in situ measured pCO_2 agree quite well over the annual cycle for the open water sector (Figure 7), suggesting that the use of the wind speed dependent transfer velocity parameterization of Nightingale et al. (2000) is largely reasonable. The variability in the implied pCO_2 (as indicated by the 25/75 percentiles), however, is sometimes greater than the variability in the in situ pCO_2. In this section, we estimate the time-varying CO_2 gas transfer velocity (K_{CO2}) and examine its variability and possible controls.

K_{CO2} is computed as flux /ΔpCO_2/sol_{CO2}, where sol_{CO2} is the solubility in CO_2. As shown in the previous section, pCO_2 measured from the open water flux footprint of PPAO is comparable to near-coincidental measurements at L4. Thus to estimate K_{CO2} for the open water sector, we combine pCO_2 measurements from the PPAO footprint with the more numerous measurements at L4. To estimate K_{CO2} for the Plymouth Sound sector, only pCO_2 measurements from that footprint are used. We linearly interpolate these seawater pCO_2 measurements to the times of the hourly CO_2 flux measurements. Interpolation more than four days away from the nearest pCO_2 observations is discarded. The interpolated pCO_2 is then combined with the measured atmospheric CO_2 mixing ratio at PPAO to yield the air-sea pCO_2 difference (ΔpCO_2). To normalize for the effect of temperature, K_{CO2} is further adjusted to the Schmidt number of 660: $K_{CO2,660} = K_{CO2} \bullet (660/Sc_{CO2})^{-0.5}$. Both the solubility and Schmidt number of CO_2 as a function of temperature and salinity are taken from Wanninkhof et al. (2014). In order to minimize any bias in the computed $K_{CO2,660}$ due to the interpolation of daytime only pCO_2 measurements (see Section 3.2), we discard the

Biogeosciences Discuss., https://doi.org/10.5194/bg-2018-503
Manuscript under review for journal Biogeosciences
Discussion started: 13 December 2018

nighttime (20:00 to 08:00 UTC) $K_{CO2,660}$ data during times of expected invasion (i.e. air-to-sea flux). The filtered hourly $K_{CO2,660}$ data are then averaged into 6-hour bins to reduce random noise.

390

5.1 Dependence of $K_{CO2,660}$ on wind speed

$K_{CO2,660}$ is plotted against the 10-m neutral wind speed (U_{10n}) in Figure 12, along with a 2rd order polynomial fit. We have retained $K_{CO2,660}$ data only when the absolute value of ΔpCO_2 exceeded 20 µatm in order to minimize errors. Further restricting data with a higher $|\Delta pCO_2|$ threshold (e.g. to 40 µatm) does not obviously reduce the scatter in the $K_{CO2,660}$ vs. wind
395 speed relationship. Error bars in $K_{CO2,660}$ are propagated from the standard errors in the fluxes. For the open water sector, $K_{CO2,660}$ shows a significant non-linear increase with wind speed ($R^2 = 0.35$, relationship significant with $p<0.0001$). The scatter in the $K_{CO2,660}$ and wind speed relationship is likely due to measurement uncertainties in flux, variability in pCO_2, as well as processes other than wind speed that affect gas exchange. $K_{CO2,660}$ for the Plymouth Sound sector will be discussed in Section 5.4.

400 The mean of the $K_{CO2,660}$ vs. wind speed relationship, as represented by the 2rd order polynomial fit, agrees (within 95% confidence interval) with the widely-used relationship derived by Nightingale et al. (2000) using the dual tracer ($^3He/SF_6$) technique. We note that more recent parameterizations of the gas transfer velocity based on $^3He/SF_6$ and radiocarbon budgets (Ho et al. 2006; Sweeney et al. 2007; Wanninkhof 2014) are largely similar to Nightingale et al. (2000). In moderate-to-high winds, measured $K_{CO2,660}$ increases with wind speed at a rate that is less than cubic – a power fit yields an exponent of 1.3. This
405 is generally consistent with other recent closed-path EC CO_2 transfer velocity measurements (Butterworth and Miller 2016, Bell et al. 2017, Blomquist et al. 2017, and Landwehr et al. 2018).

At wind speeds less than ~5 m s^{-1}, measured $K_{CO2,660}$ at the PPAO are sometimes elevated and might not be entirely representative of air-sea transfer (Yang et al. 2016a). The EC friction velocity in the open water sector (see below and in Figure S2) is also at times higher than expected at these low wind speeds. The atmosphere was often unstable when the wind speeds
410 were low (z/L of ~ -1), in part because low winds occurred more frequently during the warmer months. The Kljun et al. (2004) model predicts a flux footprint that is closer to the PPAO site during these conditions, such that the near shore environment (i.e. from the mast to the water's edge) might have a greater influence on the fluxes. Furthermore, the double rotation method used for the streamline correction of wind is known to be more uncertain at lower wind speeds. The planar fit method (Wilczak et al. 2001) may be superior under these conditions and will be an area of investigation during future PPAO flux data analyses.

415

5.2 Dependence of $K_{CO2,660}$ on friction velocity

The friction velocity (u_*), a measure of air-sea total momentum transfer, is long thought to be a more direct representation of the drivers of turbulence and gas exchange than wind speed (e.g. Csanady et al. 1990). This appears to be the case especially for moderately soluble gases that are not significantly affected by bubble-mediated gas transfer, such as dimethyl sulfide (Huebert et al. 2010; Yang et al. 2011). The relationship between $K_{CO2,660}$ and the EC u_* shows a slightly better fit (R^2 = 0.38; Figure 13) than between $K_{CO2,660}$ and U_{10n} (R^2 = 0.35). This is consistent with the idea that u_* is a more suitable predictor of $K_{CO2,660}$ than wind speed. The other benefit of relating $K_{CO2,660}$ with u_* instead of with U_{10n} is that the u_* measurement also by EC should be less affected by flow distortion than the U_{10n} measurement (Landwehr et al. 2018).

The linear fit from Landwehr et al. (2018), derived from EC measurements of CO_2 flux in the Southern Ocean, is also shown. Compared to Landwehr et al. (2018), measurements at PPAO are similar over moderate u_* values. At high u_* values (high winds), our estimates of $K_{CO2,660}$ increase with a greater power. Blomquist et al. (2017) demonstrated that waves play a role in the open ocean air-sea exchange of CO_2 at high wind speeds and we expect waves to also influence u_* (e.g. Edson et al. 2013). Waves shoal and steepen when they approach the shallower coast and generally break more frequently than over the ocean as a result of the shallower depth. $K_{CO2,660}$ measured at PPAO when waves are large might not be the same as $K_{CO2,660}$ over the open ocean. Unfortunately there were no wave measurements within the flux footprints to investigate this effect more quantitatively.

5.3 Seasonal variability in $K_{CO2,660}$

We might expect the relationship between $K_{CO2,660}$ and wind speed to vary in different seasons due to the effects of bubbles and surfactants. Woolf et al. (1997) and Leighton et al. (2017) suggested an asymmetrical gas transfer rate that is faster for invasion than for evasion due to the hydrostatic pressure effect in bubble-mediated gas exchange, which is important for CO_2 (Bell et al., 2017; Blomquist et al. 2017). Figure 12 is color-coded by ΔpCO_2 (positive when ocean is supersaturated). We see that invasion (i.e. air-to-sea) of CO_2, expected to occur in late spring and summer, was typically associated with low-to-moderate wind speeds. Evasion (i.e. sea-to-air) of CO_2, expected to occur in late autumn and winter, was typically associated with moderate-to-high wind speeds. There was limited overlap between invasion and evasion $K_{CO2,660}$ cases in the same wind speed range, partly due to gaps in the pCO_2 data. Nevertheless, many of the $K_{CO2,660}$ data were well below the polynomial fit during periods of expected evasion and when U_{10n} was between 6 and 10 m s^{-1}.

Recent measurements show large spatial and temporal differences in surfactant activity over the Atlantic ocean (Sabbaghzadeh et al. 2017). A higher surfactant activity has been associated with suppression in the gas transfer velocity (e.g. Salter et al. 2011; Pereira et al. 2016, 2018). Figure 13 is color-coded by the near surface chlorophyll a concentration (Chl *a*), an indicator of phytoplankton biomass and biological activity. Chl *a* was as low as 0.2 mg m^{-3} in the winter and early spring, and as

high as 5 mg m^{-3} during late spring and summer. Many of the $K_{CO2,660}$ data for the open water sector were below the polynomial fit at times of high Chl *a* concentration. A seasonal variability in biologically-influenced surfactant activity seems likely and could alter the $K_{CO2,660}$ vs. wind speed relationship. Higher frequency observations of pCO_2 within the flux footprint (e.g. from a buoy) would greatly increase the number of transfer velocity estimates and enable a more robust comparison between invasion and evasion. Approaches similar to Sabbaghzadeh et al. (2017) and Pereira et al. (2016) on a seasonal scale, coupled with EC gas flux measurements, would help to address the importance of naturally-produced surfactants on gas exchange.

5.4 Dependence of $K_{CO2,660}$ on bottom-driven turbulence

Gas transfer driven by bottom-driven turbulence is parameterized as by Borges et al. (2004) as: $1.719\ v^{0.5}h^{-0.5}$ (cm hr^{-1}), where v is the current velocity (in cm s^{-1}), and h is water depth (in m). The authors treated this as a linearly additive term to wind driven gas exchange. For a depth of 10 m for the Plymouth Sound and a current velocity on the order of 1 m s^{-1} during ebbing and flooding tides (Siddorn et al. 2003), we calculate a transfer velocity as a result of bottom-driven turbulence of ~5 cm hr^{-1} at a Schmidt number of 660. For the open water sector, gas transfer driven by bottom-driven turbulence is calculated to be less than 4 cm hr^{-1} due to the deeper water. For reference, the Nightingale et al. (2000) parameterization at a wind speed of 6–9 m s^{-1} is about 10–20 cm hr^{-1}. Thus bottom-driven turbulence may influence our observations of $K_{CO2,660}$ at the PPAO at low-to-moderate wind speeds. Neglecting bottom-driven turbulence when calculating implied GHG concentrations (Sections 3.3, 3.4) could have resulted in overestimates, particularly at low wind speeds. Note though that our calculations of implied GHG concentrations were limited to wind speeds >5 m s^{-1}.

$K_{CO2,660}$ derived for the Plymouth Sound sector is shown in Figures 12 and 13. Knowing the strong diurnal variability in the implied pCO_2 for this wind sector (see Figure 8), we have further limited $K_{CO2,660}$ to the time of day of 10:00 to 16:00 UTC to reduce the temporal mismatch between the flux and pCO_2 measurements. This strict filtering as well as the limited number of coincidental flux and pCO_2 measurements result in only five 6-hour $K_{CO2,660}$ estimates for the Plymouth Sound sector. These few $K_{CO2,660}$ values roughly increase with wind speed and friction velocity, and seem to be within the variability of the open water $K_{CO2,660}$ values. Note that four out of five of these $K_{CO2,660}$ estimates were associated with wind speeds over 9 m s^{-1}, for which bottom-driven turbulence is expected to have less influence (≤25% of the wind driven $K_{CO2,660}$). Future studies that combine EC flux measurements, frequent observations of seawater CO_2 and CH_4 concentrations within the Plymouth Sound footprint, and in situ measurements of current velocity would allow us to better test and improve *K* parameterizations in shallow water.

6 Conclusions

Air-sea CH_4 and CO_2 fluxes measured by eddy covariance from a coastal location in the southwest UK over one year demonstrated significant variability on seasonal timescales. CH_4 flux in the coastal seas also varied on a semi-diurnal (i.e. tidal) scale, while CO_2 flux at times varied diurnally. These observations suggest that sporadic samplings of seawater concentrations that are limited to certain seasons, times of the day, or tidal cycle could result in biased annual mean flux estimates. Surface ocean CH_4 saturations implied from the measured fluxes exceeded a few hundred percent, and were much higher over the semi-enclosed Plymouth Sound than over open water. These results are consistent with the trend in dissolved CH_4 concentration observed from the upper part of the river Tamar to the mouth of the Plymouth Sound. The coastal sea was a net sink of CO_2 in late spring and summer, and a net source of CO_2 in autumn and winter. CO_2 flux from the Plymouth Sound sector, influenced by the riverine outflow, was more positive than from the open water sector in the mean, and demonstrated greater diurnal variability. We estimated the CO_2 transfer velocity from our measurements of CO_2 fluxes and in situ seawater concentrations. In the mean, the derived CO_2 transfer velocity at this coastal location agrees reasonably well with previous tracer-based and closed-path CO_2 eddy covariance estimates from the open ocean. There are hints of seasonality in the transfer velocity vs. wind speed relationship that may be related to asymmetric bubble-mediated gas exchange or biologically derived surfactants. These effects as well as bottom-driven turbulence warrant further investigation in order to improve our understanding of air-sea gas exchange and our estimates of coastal Greenhouse Gas budgets.

Author Contribution

MY and TB designed and performed the flux measurements and data analysis. IB and AR measured dissolved CH_4 concentration, while VK measured seawater pCO_2. JF and TS supplied the underway and buoy data from the Western Channel Observatory. TS and PN provided helpful comments on the focus and context of the paper.

Acknowledgment

This work contributes to the ACSIS (The North Atlantic Climate System Integrated Study; NE/N018044/1), MOYA (Methane Observations and Yearly Assessments; NE/N015932/1), LOCATE (Land Ocean Carbon Transfer; NE/N018087/1), and CLASS (Climate Linked Atlantic Sector Science) projects funded by the Natural Environment Research Council (NERC), UK. The Western Channel Observatory is funded by NERC's National Capability programme. Trinity House (http://www.trinityhouse.co.uk/) owns the Penlee site and has kindly agreed to rent the building to PML so that instrumentation can be protected from the elements. We are able to access the site thanks to the cooperation of Mount Edgcumbe Estate (http://www.mountedgcumbe.gov.uk/). We thank the Environmental Agency for the Tamar flow data. We also thank F. E. Hopkins (PML), M. J. Yelland (National Oceanography Centre), I. M. Brooks (University of Leeds), and J. Prytherch

(Stockholm University) for continued measurement support. This is contribution number 5 from the Penlee Point Atmospheric Observatory.

References

Andersson, A.J., and Mackenzie F.T.: Shallow-water oceans: a source or sink of atmospheric CO2? Frontiers in Ecology and the Environment. 2:348-353, 2004.

Artioli, Y., Blackford, J. C., Butenschoen, M., Holt, J., Wakelin, S. L., Thomas, H., Borges, A. V., and Allen, J. I.: The carbonate system in the North Sea: Sensitivity and model validation, J. Mar. Syst., 102–104, 1–13, 2012.

Bange, H. W.: Nitrous oxide and methane in European coastal waters, Estuar. Coast. Shelf Sci., 70, 361–374, 2006.

Bell, T. G., Landwehr, S., Miller, S. D., de Bruyn, W. J., Callaghan, A. H., Scanlon, B., Ward, B., Yang, M., and Saltzman, E. S.: Estimation of bubble-mediated air–sea gas exchange from concurrent DMS and CO2 transfer velocities at intermediate–high wind speeds, Atmos. Chem. Phys., 17, 9019– 9033, https://doi.org/10.5194/acp-17-9019-2017, 2017.

Blomquist, B. W., Brumer, S. E., Fairall, C. W., Huebert, B. J., Zappa, C. J., Brooks, I. M., Yang, M., Bariteau, L., Prytherch, J., Hare, J. E., Czerski, H., Matei, A., and Pascal, R. W.: Wind Speed and Sea State Dependencies of Air-Sea Gas Transfer: Results From the High Wind Speed Gas Exchange Study (HiWinGS), Journal of Geophysical Research: Oceans, pp. n/a–n/a, https://doi.org/10.1002/2017JC013181, http://dx.doi.org/10.1002/2017JC013181, 2017.

Blomquist, B. W., Huebert, B. J., Fairall, C. W., Bariteau, L., Edson, J. B., Hare, J. E., and McGillis, W. R.: Advances in Air-Sea CO2 Flux Measurement by Eddy Correlation, Bound. -Lay. Meteorol., 152, 3, 245–276, doi:10.1007/s10546-014-9926-2, 2014.

Borges, A.V., Darchambeau, F., Teodoru, C.R., Marwick, T.R., Tamooh, F., Geeraert, N., Omengo, F.O., Guérin, F., Lambert, T., Morana, C., Okuku, E., Bouillon, S.: Globally significant greenhouse gas emissions from African inland waters. Nat. Geosci. http:// dx.doi.org/10.1038/NGEO2486, 2015.

Butterworth, B. J. and Else, B. G. T.: Dried, closed-path eddy covariance method for measuring carbon dioxide flux over sea ice, Atmos. Meas. Tech., 11, 6075-6090, https://doi.org/10.5194/amt-11-6075-2018, 2018.

Butterworth, B. J. and Miller, S. D.: Air–sea exchange of carbon dioxide in the Southern Ocean and Antarctic marginal ice zone, Geophys. Res. Lett., 43, 7223–7230, https://doi.org/10.1002/2016GL069581, 2016.

Cai, W. J., Dai, M. H., and Wang, Y. C.: Air-sea exchange of carbon dioxide in ocean margins: A province-based synthesis, Geophys. Res. Lett., 33, L12603, doi: 12610.11029/12006gl026219, doi:L12603, doi: 10.1029/2006gl026219, 2006.

Chen, C. T. A. & Borges, A. V.: Reconciling opposing views on carbon cycling in the coastal ocean: Continental shelves as sinks and near-shore ecosystems as sources of atmospheric CO2. Deep-Sea Res. Part II-Top. Stud. Oceanogr. 56, 578-590, doi:10.1016/j.dsr2.2009.01.001, 2009.

Chen, C.T.A., Huang, T.H., Chen, Y.C., Bai, Y., He, X., Kang, Y.: Air-sea exchanges of CO2 in the world's coastal seas. Biogeosciences 10, 6509-6544, 2013.

Csanady, G. T.: The role of breaking wavelets in air-sea gas transfer, J. Geophys. Res., 95, 749–759, doi:10.1029/JC095iC01p00749, 1990.

Edson, J., Hinton, A., Prada, K., Hare, J., and Fairall, C.: Direct covariance flux estimates from mobile platforms at sea, J. Atmos. Ocean. Technol., 15, 547–562, 1998.

Edson, J. B., Jampana, V., Weller, R. A., Bigorre, S. P., Plueddemann, A. J., Fairall, C. W., Miller, S. D., Mahrt, L., Vickers, D., and Hersbach H.: On the exchange of momentum over the open ocean, J. Phys. Oceanogr., 43, 1589–1610, doi:10.1175/JPO-D-12-0173.1, 2013.

Esters, L., Breivik, O., Landwehr, S., ten Doeschate, A., Sutherland, G., Christensen, K. H., Bidlot, J., and Ward B., Turbulence scaling comparisons in the ocean surface boundary layer, J. Geophys. Res., 123(3), 2172–2191, doi: 10.1002/2017JC013525, 2018.

Frankignoulle, M. and Borges, A. V.: European continental shelf as a significant sink for atmospheric carbon dioxide. Global Biogeochem. Cycles, 15, 569–576, 2001.

Frankignoulle, M., Abril, G., Borges, A., Bourge, I., Canon, C., Delille, B., Libert, E., and Theate, J.-M.: Carbon dioxide emission from European estuaries. Science 282: 434–436, 1998.

Forster G.L., Upstill-Goddard R.C., Gist N., Robinson R., Uher G., Woodward E.M.S.: Nitrous oxide and methane in the Atlantic Ocean between 501N and 521S: Latitudinal distribution and sea-to-air flux. Deep-Sea Research II 56, 964–976. doi:10.1016/j.dsr2.2008.12.002, 2009.

Gutiérrez-Loza, L. and Ocampo-Torres, F. J.: Air-sea CO2 fluxes measured by eddy covariance in a coastal station in Baja California, México, in: IOP Conference Series: Earth and Environmental Science, vol. 35, p. 012012, IOP Publishing, 2016.

Hartmann, D.L., A.M.G. Klein Tank, M. Rusticucci, L.V. Alexander, S. Brönnimann, Y. Charabi, F.J. Dentener, E.J. Dlugokencky, D.R. Easterling, A. Kaplan, B.J. Soden, P.W. Thorne, M. Wild and P.M. Zhai, 2013: Observations: Atmosphere and Surface. In: Climate Change 2013: The Physical Science Basis. Contribution of Working Group I to the Fifth Assessment Report of the Intergovernmental Panel on Climate Change [Stocker, T.F., D. Qin, G.-K. Plattner, M. Tignor, S.K. Allen, J. Boschung, A. Nauels, Y. Xia, V. Bex and P.M. Midgley (eds.)]. Cambridge University Press, Cambridge, United Kingdom and New York, NY, USA, 2013.

Helmig, D., Rossabi, S., Hueber, J., Tans, P., Montzka, S. A., Masarie, K., Thoning, K., Plass-Duelmer, C., Claude, A., Carpenter, L. J., Lewis, A. C., Punjabi, S., Reimann, S., Vollmer, M. K., Steinbrecher, R., Hannigan, J. W., Emmons, L. K., Mahieu, E., Franco, B., Smale, D., and Pozzer, A.: Reversal of global atmospheric ethane and propane trends largely due to US oil and natural gas production, Nat. Geosci., 9, 490–495, https://doi.org/10.1038/ngeo2721, 2016.

Ho, D. T., Ferrón, S., Engel, V. C., Larsen, L. G., and Barr, J. G.: Air-water gas exchange and CO2 flux in a mangrove-dominated estuary, Geophys. Res. Lett., 41, doi:10.1002/2013GL058785, 2014.

Ho, D. T., Law, C. S., Smith, M. J., Schlosser, P., Harvey, M., and Hill, P.: Measurements of air-sea gas exchange at high wind speeds in the Southern Ocean: Implications for global parameterizations Geophys. Res. Let. 33:L16611, doi:10. 1029/2006GL026817, 2006.

Honkanen, M., Tuovinen, J.-P., Laurila, T., Mäkelä, T., Hatakka, J., Kielosto, S., and Laakso, L.: Measuring turbulent CO_2 fluxes with a closed-path gas analyzer in a marine environment, Atmos. Meas. Tech., 11, 5335-5350, https://doi.org/10.5194/amt-11-5335-2018, 2018.

Houghton, R. A. in Treatise on Geochemistry Vol. 8 (eds W.H. Schlesinger, H.D. Holland, & K.K. Turekian), 473-513, Elsevier, 2003.

Huebert, B., Blomquist, B., Yang, M., Archer, S., Nightingale, P., Yelland, M., Stephens, J., Pascal, R., and Moat, B.: Linearity of DMS transfer coefficient with both friction velocity and wind speed in the moderate wind speed range, Geophys. Res. Lett., 37, L01605, doi:10.1029/ 2009GL041203, 2010.

Khatiwala, S. et al. Global ocean storage of anthropogenic carbon. Biogeosciences 10, 2169-2191, doi:10.5194/bg-10-2169-2013, 2013.

Kitidis, V., Hardman-Mountford, N.J., Litt, E., Brown, I., Cummings, D., Hartman, S., Hydes, D., Fishwick, J.R., Harris, C., Martinez-Vicente, V., Malcolm, E., Woodward, S., Smyth, T.J.: Seasonal dynamics of the carbonate system in the Western English Channel. Cont. Shelf Res. 42, 30–40, 2012.

Kitidis, V., Tizzard, L., Uher, G., Judd, A., Upstill-Goddard, R.C., Head, I.M., Gray, N.D., Taylor, G., Duran, R., Diez, R., Iglesias, J., Garcia-Gil, S.: The biogeochemical cycling of methane in Ria de Vigo, NW Spain: Sediment processing and sea-air exchange. J. Mar. Syst. 66, 258-271, 2007.

Kljun, N., Calanca, P., Rotach, M.W., Schmid, H.P.:A Simple Parameterisation for Flux Footprint Predictions, Boundary-Layer Meteorology, 112, 503-523, 2004.

Landwehr, S., Miller, S. D., Smith, M. J., Bell, T. G., Saltzman, E. S., and Ward, B.: Using eddy covariance to measure the dependence of air–sea CO_2 exchange rate on friction velocity, Atmos. Chem. Phys., 18, 4297-4315, https://doi.org/10.5194/acp-18-4297-2018, 2018.

Landwehr, S., Miller, S. D., Smith, M. J., Saltzman, E. S., and Ward, B.: Analysis of the PKT correction for direct CO2 flux measurements over the ocean, Atmos. Chem. Phys., 14, 3361–3372, doi:10.5194/acp-14-3361-2014, 2014.

Laruelle, G. G., Durr, H. H., Slomp, C. P., and Borges, A. V: Evaluation of sinks and sources of CO2 in the global coastal ocean using a spatially-explicit typology of estuaries and continental shelves. Geophysical Research Letters 37, doi: 10.1029/2010gl043691, 2010.

Le Quéré, C., Moriarty, R., Andrew, R.M., Peters, G.P., Ciais, P., Friedlingstein, P., Jones, S.D., Sitch, S., Tans, P., Arneth, A., Boden, T.A., Bopp, L., Bozec, Y., Canadell, J.G., Chevallier, F., Cosca, C.E., Harris, I., Hoppema, M., Houghton, R.A., House, J.I., Jain, A., Johannessen, T., Kato, E., Keeling, R.F., Kitidis, V., Goldewijk, K.K., Koven, C., Landa, C.S., Landschützer, P., Lenton, A., Lima, I.D., Marland, G., Mathis, J.T., Metzl, N., Nojiri, Y., Olsen, A., Ono, T., Peters, W., Pfeil, B., Poulter, B., Raupach, M.R., Regnier, P., Rödenbeck, C., Saito, S., Salisbury, J.E., Schuster, U., Schwinger, J., Séférian, R., Segschneider, J., Steinhoff, T., Stocker, B.D., Sutton, A.J., Takahashi, T., Tilbrook, B., Werf, G.R.v.d., Viovy, N., Wang, Y.-P., Wanninkhof, R., Wiltshire, A., Zeng, N.: Global carbon budget 2014, Earth System Science Data 7, 47-85, 2015.

Leighton, T., Coles, D.G.H., Srokosz, M., White, P.R., and Woolf, D.K.: Asymmetric transfer of CO2 across a broken sea surface, Nature Scientific Reports, DOI:10.1038/s41598-018-25818-6, 2018.

Litt, E.J., Hardman-Mountford, N.J., Blackford, J.C., Mitchelson-Jacob, G., Goodman, A., Moore, G.F., Cummings, D.G., Butenschon, M.: Biological control of pCO2 at station L4 in the Western English Channel over 3 years. Journal of Plankton Research 32, 621–629, 2010.

Marrec, P., et al., Spatio-temporal dynamics of biogeochemical processes and air–sea CO2 fluxes in the Western English Channel based on two years of FerryBox deployment, J. Mar. Syst., http://dx.doi.org/10.1016/j.jmarsys.2014.05.010, 2014.

Middelburg, J.J., Nieuwenhuize, J., Iversen, N., Høgh, N., De Wilde, H., Helder, W., Seifert, R., Christof, O.: Methane distribution in European tidal estuaries. Biogeochemistry, 59, 95e119, 2002.

Moat, B.J., Yelland, M. J., Pascal, R. W., and Molland, A. F.: An overview of the airflow distortion at anemometer sites on ships. Int. J. Climatol., 25, 997–1006, 2005.

Muller-Karger, F. E., Varela, R. Thunell, R. Luerssen, R., Hu, C. and Walsh J. J.: The importance of continental margins in the global carbon cycle, Geophys. Res. Lett., 32, L01602, doi:10.1029/2004GL021346, 2005.

Nightingale P.D., Malin G, Law C.S., Watson A.J., Liss P.S., Liddicoat M.I., Boutin J, Upstill-Goddard R.C.: In situ evaluation of air–sea gas exchange parameterizations using novel conservative and volatile tracers. Glob Biogeochem Cycles 14:373–387. 2000.

Nisbet, E.G., Dlugokencky, E. J., Manning, M. R., Lowry, D., Fisher, R. E., France, J. L., Michel, S. E., Miller, J. B., White, J. W. C., Vaughn, B., Bousquet, P., Pyle, J. A., Warwick, N. J., Cain, M., Brownlow, R., Zazzeri, G., Lanoisellé, M., Manning, A. C., Gloor, E., Worthy, D. E. J., Brunke, E.-G., Labuschagne, C., Wolff, E. W., and Ganesan, A. L.: Rising atmospheric methane: 2007-2014 growth and isotopic shift, Global Biogeochem. Cy., 30, 1356–1370, doi:10.1002/2016GB005406, 2016.

O'Connor, D. J., and W. E. Dobbins, Mechanism of reaeration in natural streams, Trans. Am. Soc. Civ. Eng., 123, 641–684, 1958.

Pereira, R., Schneider-Zapp, K., and Upstill-Goddard, R. C.: Surfactant control of gas transfer velocity along an offshore coastal transect: results from a laboratory gas exchange tank, Biogeosciences, 13, 3981-3989, https://doi.org/10.5194/bg-13-3981-2016, 2016.

Pereira, R., Ashton, I., Sabbaghzadeh, B., Shutler, J.D., Upstill-Goddard, R.C.: Reduced air–sea CO2 exchange in the Atlantic Ocean due to biological surfactants, Nature Geoscience, 11, 492–496, https://doi.org/10.1038/s41561-018-0136-2, 2018.

Rigby, M., Montzka, S. A., Prinn, R. G., White, J. W. C., Young, D., O'Doherty, S., Lunt, M. F., Ganesan, A. L., Manning, A. J., Simmonds, P. G., Salameh, P. K., Harth, C. M., Mühle, J., Weiss, R. F., Fraser, P. J., Steele, L. P., Krummel, P. B., Mc- Culloch,

A., and Park, S.: Role of atmospheric oxidation in recent methane growth, P. Natl. Acad. Sci., 114, 5373–5377, https://doi.org/10.1073/pnas.1616426114, 2017.

Pison, I., Ringeval, B., Bousquet, P., Prigent, C., and Papa, F.: Stable atmospheric methane in the 2000s: key-role of emissions from natural wetlands, Atmos. Chem. Phys., 13, 11609–11623, https://doi.org/10.5194/acp-13-11609-2013, 2013.

Rice AL, et al.: Atmospheric methane isotopic record favors fossil sources flat in 1980s and 1990s with recent increase. Proc Natl Acad Sci USA 113:10791–10796, 2016.

Rutgersson, A., Norman, M., Schneider, B., Pettersson, H., Sahlée, E.: The annual cycle of carbon dioxide and parameters influencing the air–sea carbon exchange in the Baltic Proper. J. Mar. Syst. 74, 381–394, 2008.

Sabbaghzadeh, B., Upstill-Goddard, R. C., Beale, R., Pereira, R., and Nightingale, P. D.: The Atlantic Ocean surface microlayer from 50°N to 50°S is ubiquitously enriched in surfactants at wind speeds up to 13m s^{-1}. Geophys. Res. Lett. 44, 2852–2858. doi: 10.1002/2017GL072988, 2017.

Salter, M. E., Upstill-Goddard, R. C., Nightingale, P. D., Archer, S. D., Blomquist, B., Ho, D. T., Huebert, B., Schlosser, P., and Yang, M.: Impact of an artificial surfactant release on air-sea gas fluxes during Deep Ocean Gas Exchange Experiment II, J. Geo- phys. Res.-Oceans, 116, C11016, doi:10.1029/2011JC007023, 2011.

Schaefer, H., et al.: A 21st century shift from fossil-fuel to biogenic methane emissions indicated by 13CH4, Science, 352, 80–84, 2016.

Siddorn, J.R., Allen, J.I. and Uncles, R.J: Heat, salt and tracer transport in the Plymouth Sound coastal region: a 3-D modelling study, J. Mar. Biol. Ass. U.K., 83, 673-682, 2003.

Sims, R. P., Schuster, U., Watson, A. J., Yang, M. X., Hopkins, F. E., Stephens, J., and Bell, T. G.: A measurement system for vertical seawater profiles close to the air–sea interface, Ocean Sci., 13, 649-660, https://doi.org/10.5194/os-13-649-2017, 2017.

Sweeney, C., et al.: Constraining global air-sea gas exchange for CO2 with recent bomb C-14 measurements. Global Biogeochem. Cycles 21:GB2015, doi:10.1029/2006GB002784, 2007.

Tanner, C. B. and Thurtell, G. W.: Anemoclinometer Measurements of Reynolds Stress and Heat Transport in the Atmospheric Surface Layer, University of Wisconsin Tech. Rep., ECOM-66-G22- F, 82 pp., 1969.

Upstill-Goddard, R. C., et al.: Simultaneous high-precision measurements of methane and nitrous oxide in water and seawater by single phase equilibration gas chromatography, Deep-Sea Research Part I-Oceanographic Research Papers, *43*, 1669-1682, 1996.

Upstill-Goddard, R. C.: Air-sea gas exchange in the coastal zone. Estuar. Coast. Shelf Sci. 70, 388-404, 2006.

Upstill-Goddard, R. C., Barnes, J., Frost, T., Punshon, S., Owens, N.J.P.: Methane in the southern North Sea: low-salinity inputs, estuarine removal, and atmospheric flux. Global Biogeochemical Cycles 14, 1205e1217, 2000.

Upstill-Goddard, R. C., Barnes, J.: Methane emissions from UK estuaries: Re-evaluating the estuarine source of tropospheric methane from Europe, Marine Chemistry, doi: 10.1016/j.marchem.2016.01.010 , 2016.

Wanninkhof, R., Asher, W. E., Ho, D. T., Sweeney, C. S., and McGillis, W. R.: Advances in quantifying air-sea gas exchange and environmental forcing. Ann. Rev. Mar. Sci- ence 1:213-244, 2009.

Wilczak, J., Oncley, S., and Stage, S.: Sonic anemometer tilt correction algorithms, Bound.-Lay. Meteorol., 99, 127–150, https://doi.org/10.1023/A:1018966204465, 2001.

Yang, M., Nightingale, P., Beale, R., Liss, P., Blomquist, B., and Fairall, C.: Atmospheric deposition of methanol over the Atlantic Ocean, P. Natl. Acad. Sci., doi:10.1073/pnas.1317840110, 110, 20034–20039, 2013.

Wanninkhof, R.: Relationship between wind speed and gas exchange over the ocean revisited. Limnology Oceanography: Methods, 12, 351–362. https://doi.org/10.4319/lom.2014.12.351, 2014.

Woolf, D. K.: Bubbles and their role in gas exchange, in The Sea Surface and Global Change, edited by R. Duce and P. Liss, pp. 173–205, Cambridge Univ. Press, New York, doi:10.1017/CBO9780511525025.007, 1997.

Yang, M., Blomquist, B. W., Fairall, C. W., Archer, S. D., and Hue- bert, B. J.: Air-sea exchange of dimethylsulfide in the Southern Ocean: Measurements from SO GasEx compared to temper- ate and tropical regions, J. Geophys. Res.-Oceans, 116, C00F05, doi:10.1029/2010jc006526, 2011.

Yang, M., Bell, T. G., Hopkins, F. E., Kitidis, V., Cazenave, P. W., Nightingale, P. D., Yelland, M. J., Pascal, R. W., Prytherch, J., Brooks, I. M., and Smyth, T. J.: Air–sea fluxes of CO_2 and CH_4 from the Penlee Point Atmospheric Observatory on the south-west coast of the UK, Atmos. Chem. Phys., 16, 5745-5761, https://doi.org/10.5194/acp-16-5745-2016, 2016a.

Yang, M., Prytherch, J., Kozlova, E., Yelland, M. J., Parenkat Mony, D., and Bell, T. G.: Comparison of two closed-path cavity-based spectrometers for measuring air–water CO_2 and CH_4 fluxes by eddy covariance, Atmos. Meas. Tech., 9, 5509-5522, https://doi.org/10.5194/amt-9-5509-2016, 2016b.

Biogeosciences Discuss., https://doi.org/10.5194/bg-2018-503
Manuscript under review for journal Biogeosciences
Discussion started: 13 December 2018

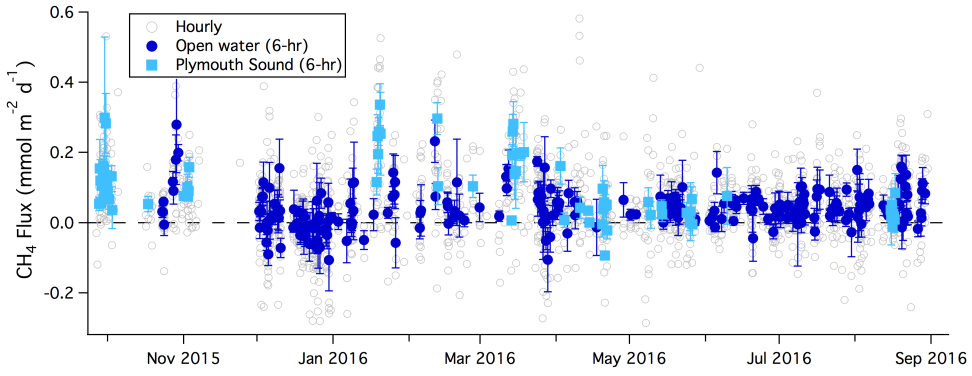

Figure 1. One-year time series of CH_4 flux (hourly average) during times when winds were from the sea. Six-hour averages of fluxes are further separated into the open water (southwest) and Plymouth Sound (northeast) wind sectors. Error bars indicate standard error.

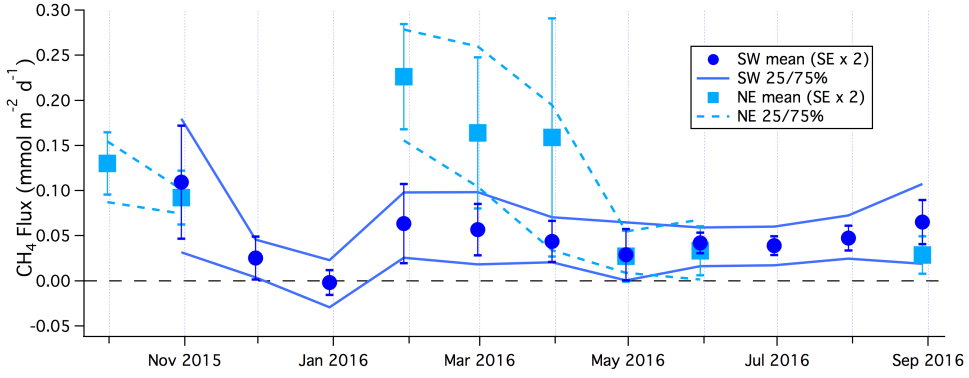

Figure 2. Monthly averages and 25/75 percentiles of CH_4 flux from the open water (southwest) and Plymouth Sound (northeast) wind sectors. Error bars indicate 2 times standard error.

Biogeosciences Discuss., https://doi.org/10.5194/bg-2018-503
Manuscript under review for journal Biogeosciences
Discussion started: 13 December 2018

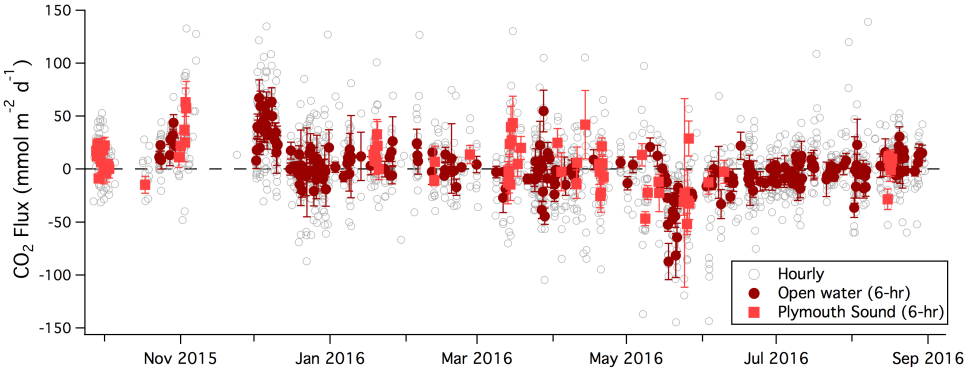

Figure 3. One-year time series of CO_2 flux (hourly average) during times when winds were from the sea. Six-hour averages are further separated into the open water (southwest) and Plymouth Sound (northeast) wind sectors. Error bars indicate standard error.

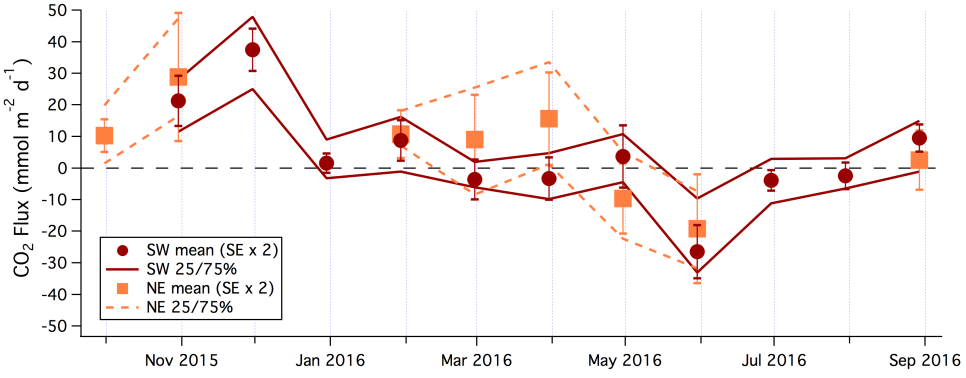

Figure 4. Monthly averages and 25/75 percentiles of CO_2 flux from the open water (southwest) and Plymouth Sound (northeast) wind sectors. Error bars indicate 2 times standard error.

Biogeosciences Discuss., https://doi.org/10.5194/bg-2018-503
Manuscript under review for journal Biogeosciences
Discussion started: 13 December 2018

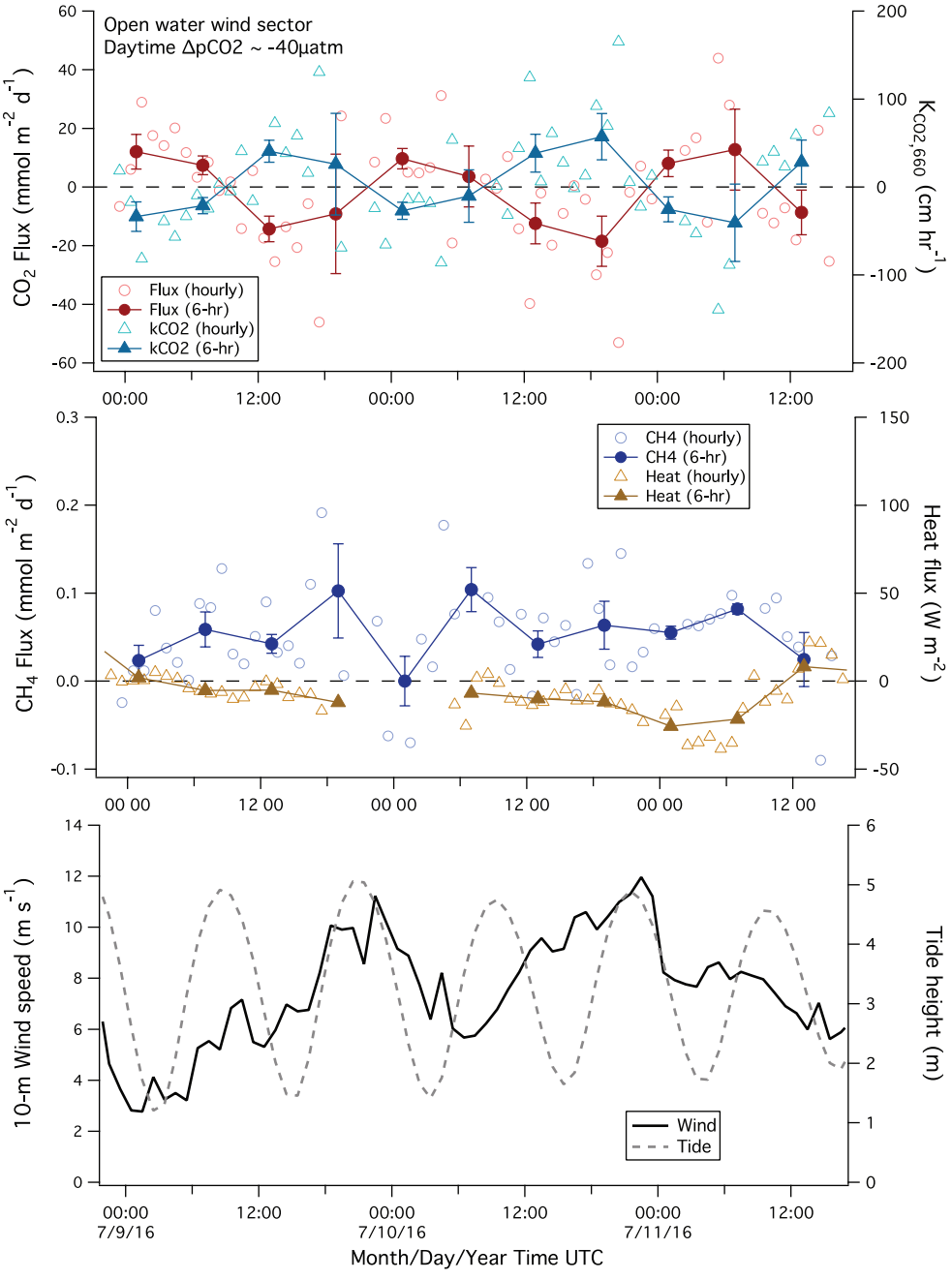

Figure 5. Example of variability in A) CO_2 flux and computed transfer velocity, B) CH_4 flux and sensible heat flux, and C) wind speed and tidal height. Fluxes are shown in both hourly and 6-hr averages. Gaps in heat flux data were due to heavy rain, which does not significantly affect the gas flux measurement.

Biogeosciences Discuss., https://doi.org/10.5194/bg-2018-503
Manuscript under review for journal Biogeosciences
Discussion started: 13 December 2018

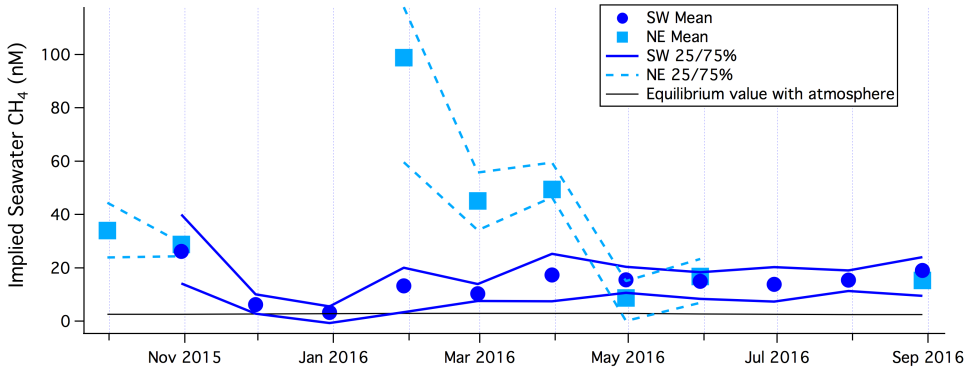

Figure 6. Monthly averages and 25/75 percentiles of implied CH_4 concentration in the surface waters within the EC flux footprint, along with the equilibrium value with respect to the atmosphere.

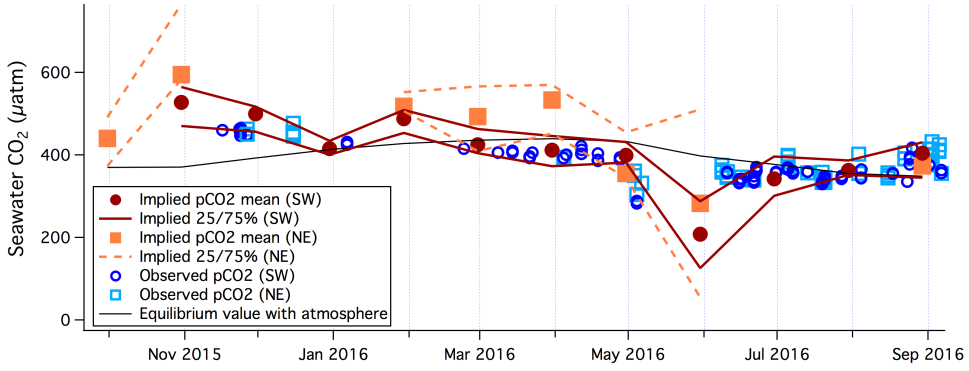

Figure 7. Monthly averages and 25/75 percentiles of implied CO_2 concentration in the surface waters within the EC flux footprint. Observed pCO_2 from the Plymouth Quest within the southwest open water sector (plus at L4) and within the Plymouth Sound sector are also shown, along with the equilibrium value with respect to the atmosphere.

Biogeosciences Discuss., https://doi.org/10.5194/bg-2018-503
Manuscript under review for journal Biogeosciences
Discussion started: 13 December 2018

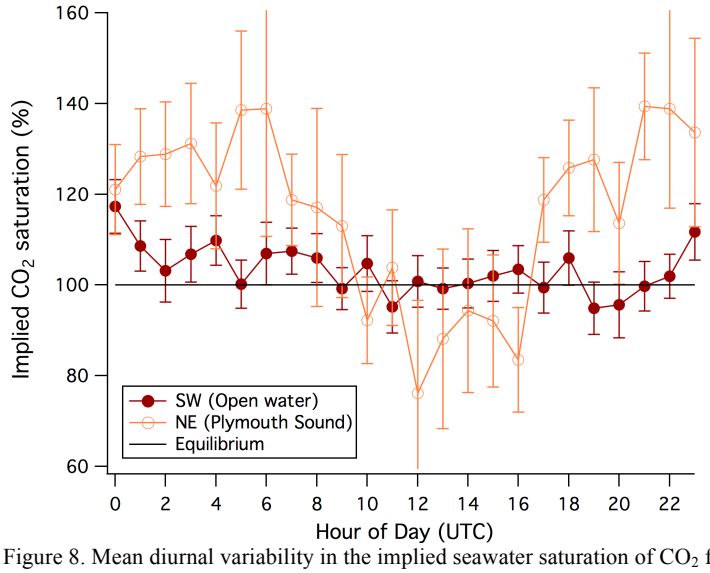

Figure 8. Mean diurnal variability in the implied seawater saturation of CO_2 for the open water (southwest) sector and the Plymouth Sound (northeast) sector. Error bars indicate standard errors.

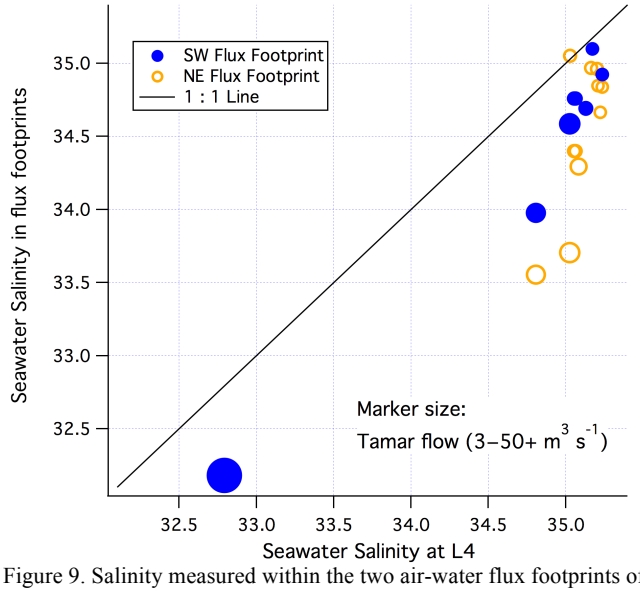

Figure 9. Salinity measured within the two air-water flux footprints of Penlee vs. near-coincidental measurements from the *Quest* at the L4 station. The size of the markers corresponds to the flow rate in the estuary Tamar, as measured at Gunnislake.

Biogeosciences Discuss., https://doi.org/10.5194/bg-2018-503
Manuscript under review for journal Biogeosciences
Discussion started: 13 December 2018

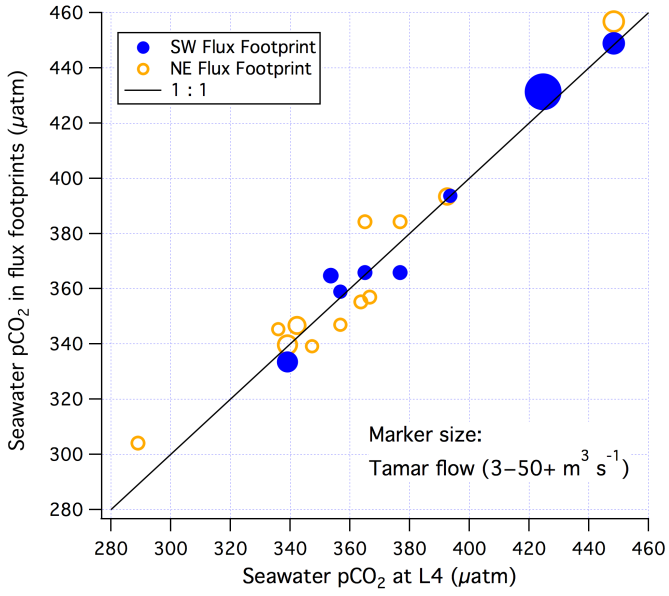

Figure 10. pCO_2 measured within the two air-water flux footprints of Penlee vs. near-coincidental measurements from the *Quest* at the L4 station. The size of the markers corresponds to the flow rate in the estuary Tamar, as measured at Gunnislake.

850

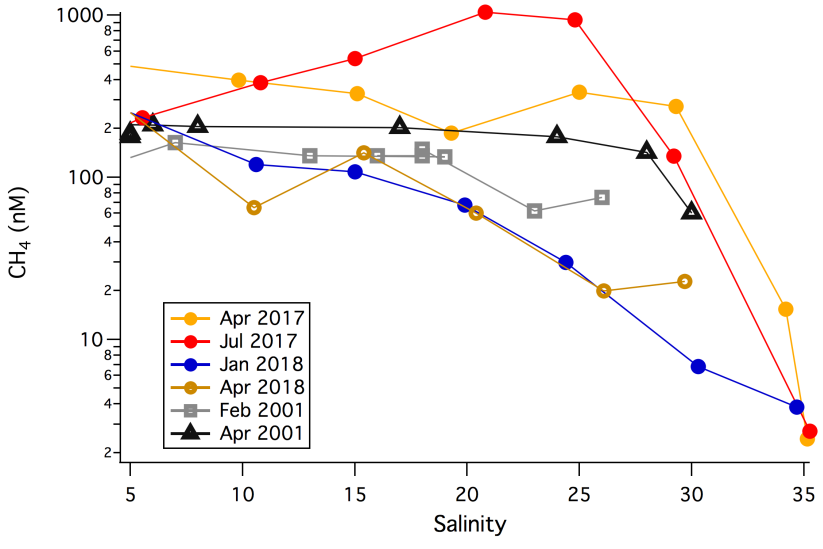

Figure 11. Dissolved CH_4 concentration from the estuary Tamar varies with salinity. Data from 2017 and 2018 are a part of the LOCATE sampling. The 2001 data are taken from Upstill-Goddard et al. (2016).

855

Biogeosciences Discuss., https://doi.org/10.5194/bg-2018-503
Manuscript under review for journal Biogeosciences
Discussion started: 13 December 2018

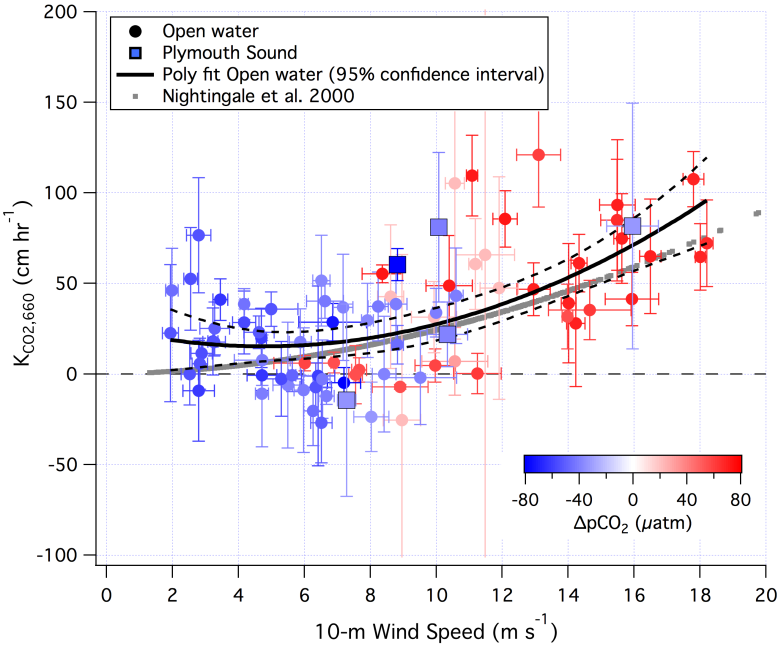

Figure 12. CO_2 transfer velocity (normalized to a Schmidt number of 660) vs. 10-m neutral wind speed for both the open water and the Plymouth Sound wind sectors. Note that color-coding is capped at $|\Delta pCO_2|$ values of 80 µatm for clarity.

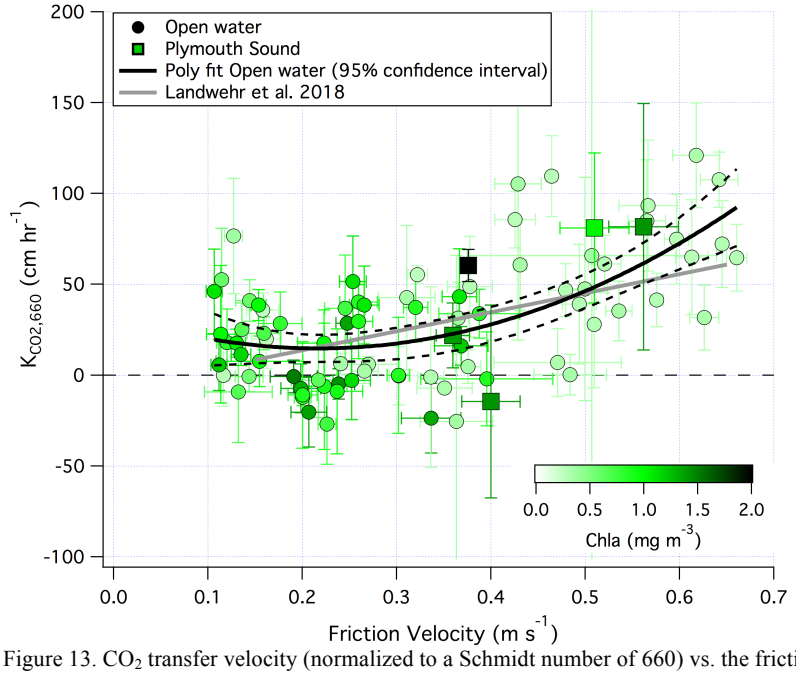

Figure 13. CO_2 transfer velocity (normalized to a Schmidt number of 660) vs. the friction velocity for both the open water and the Plymouth Sound wind sectors. Note that color-coding is capped at a chlorophyll a concentration of 2 mg m^{-3} for clarity.